

# Kinetics of molecular hydrogen dissociative adsorption on Si(111) studied by sum-frequency vibrational spectroscopy and second harmonic generation

M. Y. Mao, P. B. Miranda,\* D. S. Kim,† and Y. R. Shen‡

*Department of Physics, University of California, Berkeley, California 94720*

*and Materials Sciences Division, Lawrence Berkeley National Laboratory, Berkeley, California 94720*

(Received 19 September 2000; published 26 June 2001)

Sum-frequency vibrational spectroscopy (SFVS) and optical second-harmonic generation (SHG) were used to monitor hydrogen adsorption on Si(111) by molecular-hydrogen dosing. A properly treated sample exhibited a single H-Si stretch-vibrational mode representing H adsorbed at the top sites. A fully H-terminated Si(111) surface could be obtained by H<sub>2</sub> dosing at sufficiently high temperatures. The observed adsorption kinetics was qualitatively the same as that reported by Höfer and co-workers, including a nearly equal adsorption-energy barrier. However, our results indicate that the initial adsorption on a nearly bare surface obeys the simple Langmuir model. And with subsequent adsorption to higher coverage range, the adsorption gradually becomes cooperative type with the sticking coefficient increasing with H coverage at sufficient high temperature. Evidences of SFVS spectroscopy revealed that it is related to the Si(111) surface-structure change during H<sub>2</sub> adsorption, which appeared to undergo a structural change from (7×7) to (1×1) with increasing temperature or coverage. A simple model was used to qualitatively explain our observation.

DOI: 10.1103/PhysRevB.64.035415

PACS number(s): 68.43.Mn, 68.49.Uv, 51.70.+f

## I. INTRODUCTION

Hydrogen adsorption on Si(111) is a problem that has been extensively studied.<sup>1–13</sup> For decades, atomic H dosing was the accepted scheme to prepare H-terminated Si surfaces,<sup>1–10</sup> but the resulting surface often has many structural defects.<sup>10</sup> In 1990, the NH<sub>4</sub>F-based wet-chemical-etching method was found to be able to provide atomically flat, ideally H-terminated Si(111)-(1×1) surfaces.<sup>14,15</sup> More recently, an alternative way of preparing H-covered Si surfaces by molecular-hydrogen dosing has been proposed and investigated.<sup>11–13,16,17</sup> Hydrogen adsorption on Si by molecular-hydrogen dosing is a dissociative adsorption process. It is known that the sticking coefficient of H in such a process is extremely low at room temperature, and therefore the process was not considered useful for preparing H-terminated Si surfaces in practice. However, Höfer and co-workers<sup>11,12,18</sup> discovered that the sticking coefficient increases rapidly with temperature. Dosing of H<sub>2</sub> at a sufficiently high substrate temperature can yield a fully covered H-terminated Si(111) surface with a quality as good as the one prepared by the wet-chemical-etching method.<sup>13</sup> Molecular-hydrogen dosing on Si is relevant to the Si growth process in chemical-vapor deposition. Scientifically, as a problem of fundamental interest, it has attracted a great deal of attention.<sup>11–13,16–20</sup> The low sticking coefficient for H<sub>2</sub> dissociative adsorption at room temperature suggested that there should exist a significant adsorption-energy barrier, which was found by Bratu and co-workers to be 0.9 eV.<sup>11,12</sup> One would expect that in H<sub>2</sub> recombinative desorption from Si, the same barrier would yield a large excess kinetic energy in the desorbing H<sub>2</sub>, but this was not observed.<sup>9</sup> Höfer and co-workers showed, from the result of temperature-dependent sticking coefficient, that H<sub>2</sub> dissociative adsorption must be a phonon-assisted process, with H<sub>2</sub> desorption appearing naturally as a reverse process.<sup>18</sup> Theoretical mod-

els by Vittadini and Selloni<sup>19</sup> and Cho, Kaxiras, and Joannopoulos<sup>20</sup> suggested that on adsorption, thermal back-bond breaking would allow the adatom to move toward the incoming H<sub>2</sub> molecule and facilitate the formation of two surface Si-H bonds. On desorption, two neighboring adsorbed H atoms would recombine and desorb, leaving the Si atom dangling in an excited vibrational state.

In the work of Höfer and co-workers, the Si surfaces were prepared and characterized following the usual scheme and H coverage on Si was monitored by optical second-harmonic generation (SHG).<sup>11,12,18</sup> We have found that the conventional techniques, such as low-energy electron diffraction (LEED), often do not have enough sensitivity to assess the quality of a crystalline surface, i.e., to reveal strains and defects on the surface. Sum-frequency vibrational spectroscopy (SFVS), on the other hand, can provide a surface vibrational spectrum that directly reflects the surface quality, at least around the H-adsorption sites. With this spectroscopic technique, we have observed that the quality of a H-terminated Si(111) surface does depend critically on how the surface is prepared.<sup>13</sup> Specifically, for surfaces prepared by H<sub>2</sub> dosing, it depends on the flash-cleaning procedure of the bare Si surface. We then wonder if the kinetics of H<sub>2</sub> dissociative adsorption is different on differently prepared surfaces. This motivates us to repeat the study of Höfer and co-workers on the kinetics of H<sub>2</sub> dissociative adsorption on Si(111) characterized by SFVS spectroscopy.

In our experiment, we relied on the spectral profile of the Si-H stretch vibration in the SFVS spectrum to find the proper procedure for sample preparation that would yield a satisfactory surface quality. We found that in our case, only when the bare Si(111) surface had been cleaned by flash heating at 1500 K or higher, was the surface quality of the H/Si(111) obtained from H<sub>2</sub> dosing as good as that from wet-chemical etching. We then used SHG to monitor *in situ* the surface coverage of H, as in the case of Höfer and co-

workers. Our results on the adsorption kinetics agree in general with those obtained by Höfer and co-workers, but differ in some details. This is remarkable considering that in the past the initial sticking coefficients of  $H_2$  on Si(111) or Si(100) obtained by different groups could differ by several orders of magnitude (to be discussed further in Sec. III E). The main difference between our results and those of Höfer and co-workers is that our measured sticking coefficient increases with H coverage only at certain higher coverage range. At lower H coverage, we observed a Langmuir-type adsorption behavior in which the sticking coefficient decreases with increase of coverage. To explain our observation qualitatively, we propose a model based on a surface-structural change induced by adsorption-assisted removal of adatoms on the surface. We did observe in SHG and SFVS the evidence of surface-structural change during adsorption.

## II. EXPERIMENTAL ARRANGEMENT

### A. Sample preparation

The Si(111) samples ( $20 \times 5 \times 0.25 \text{ mm}^3$  in dimension) used in our work were cut from Boron-doped Si wafers. Their resistivity was in the range of  $0.005\text{--}0.2 \text{ } \Omega \text{ cm}$ , suitable for resistive heating of the samples. One of the difficulties in the experiment was in the accuracy of temperature measurement. A thermocouple attached to the back surface of a sample is the method commonly adopted for temperature measurement of a sample situated in an ultrahigh vacuum (UHV) chamber. In our case, however,  $H_2$  dosing had a cooling effect on the Si sample, depending on the gas pressure. We found that a thermocouple attached to the sample was generally too slow in response to the pressure variation and measured an appreciably lower temperature. To solve this problem, we resorted to a new way of attaching a thermometer to a Si sample. Thermal oxidation first led to the growth of a  $3\text{-}\mu\text{m}$ -thick  $\text{SiO}_2$  layer on the Si sample surfaces. A  $100\text{-nm}$ -thick tungsten film was then sputtered on the back surface, and photolithography/etching was used to obtain a serpentine-shaped  $50\text{-}\mu\text{m}$ -wide tungsten-wire thermistor covering an area of  $5 \times 3.5 \text{ mm}^2$  at the center. An additional  $0.5\text{-}\mu\text{m}$ -thick  $\text{SiO}_2$  layer was sputtered over the tungsten resistor in order to protect it from being etched away in the later chemical etching process.

To prepare the front surface for measurements, we wet treated the sample chemically before loading it into a UHV chamber. First, with the back surface covered, it was dipped into a buffered HF solution ( $\text{HF}:\text{NH}_4\text{F} = 1:7$ ) to remove the  $\text{SiO}_2$  layer present at the front surface. It was then reoxidized in  $\text{HCl}/\text{H}_2\text{O}_2$  (1:4) solution at  $80^\circ\text{C}$  for 10 min. Finally, it was immersed in a 40%  $\text{NH}_4\text{F}$  solution for 3 to 5 min, followed by rinsing with deionized water and blowing dry. This treatment provided an ideally H-terminated Si(111)-( $1 \times 1$ ) surface with an atomic-scale smoothness.<sup>21</sup>

After the wet-chemical treatment, the sample was immediately loaded into a UHV chamber with a base pressure of  $5 \times 10^{-10}$  Torr. It was mounted on a stage by two titanium clamps through which a dc current could be applied to resistively heat the sample. The sample temperature was obtained by measuring the resistance of the tungsten thermistor. Since

the thermistor was a thin-film wire directly coated on the back surface behind the spot to be interrogated by the laser probe, it had a fast response to laser heating and gas cooling of the front surface. It allowed accurate temperature measurements or maintenance at constant temperature through feedback control needed for the experiment in varying environment. The tungsten thermistor was precalibrated against a thermocouple attached to the front sample surface. In the temperature range of  $420\text{--}1000 \text{ K}$ , its sensitivity was about  $1.6 \text{ } \Omega/\text{K}$ . The sample temperature in our experiment could be controlled to within a few degrees and the accuracy of the absolute temperature was better than  $15 \text{ K}$ . In the higher temperature range ( $>1050 \text{ K}$ ), the sample temperature was also measured by an optical pyrometer with an accuracy of  $30 \text{ K}$ .

For surface cleaning, the sample in UHV was first resistively heated at  $900 \text{ K}$  for a few hours and then flashed to a high temperature ( $\sim 1220 \text{ K}$ ) a few times to completely degas the sample and the clamps. It was further flash heated to a higher temperature as the last step of surface cleaning. The commonly adopted cleaning procedure is to heat the sample to  $\sim 1300 \text{ K}$  for 1–2 min, followed by a slow cooling ( $<2 \text{ K/s}$ ) process.<sup>11,18,22</sup> We used a procedure adopted by some researchers that requires flash heating the sample to  $\sim 1500 \text{ K}$  for 20–30 s,<sup>23–25</sup> followed by a more rapid cooling ( $\sim 50 \text{ K/s}$ ) process.<sup>13</sup> In both cases, a sharp ( $7 \times 7$ ) LEED pattern characterizing the surface was observed, and no surface contamination could be detected by Auger spectroscopy. However, as we shall describe in Sec. III A, the latter procedure appears to yield H-terminated Si(111) surfaces with better quality from molecular-hydrogen dosing, judging from the SFVS spectra.<sup>13</sup> A recent STM study showed that the high-temperature flash treatment leads to a better ordered ( $7 \times 7$ ) surface, at least in the terrace region.<sup>10</sup>

### B. Molecular-hydrogen dosing

For  $H_2$  dosing, the UHV chamber was back filled with  $H_2$  through a leak valve. Ultrapure  $H_2$  (99.999%) gas was used. Before going into the chamber, it was further purified by passing through a  $50\text{-m}$ -long, liquid-nitrogen-cooled, copper-tubing coil to filter out the residual impurities. With this setup, the  $H_2$  pressure could be raised to as high as 10 Torr without measurable contamination on the sample surface. The  $H_2$  pressure was measured by a well-calibrated thermocouple gauge and a capacitor gauge with an absolute accuracy of  $\sim 10\%$ . To avoid contamination of the sample, all hot filaments in the UHV chamber were turned off during  $H_2$  dosing. The  $H_2$  dissociative adsorption kinetics was studied in the temperature range of  $400\text{--}1000 \text{ K}$  and gas pressure range of  $10^{-3}\text{--}10$  Torr. The  $H_2$  exposure of the sample was varied by the gas pressure and exposure time. The maximum was  $\sim 3 \times 10^4$  Torr sec (or  $3 \times 10^{10}$  Langmuir units).

### C. SHG and SFVS for measurements of H surface coverage

The theory and experimental arrangement of SHG and SFVS as *in situ* surface probes have been described elsewhere.<sup>26,27</sup> Here we give only a very brief account. A picosecond Nd:YAG laser and optical parametric system

generated coherent output beams of fixed wavelengths at 1.06 and 0.53  $\mu\text{m}$  as well as tunable infrared wavelengths down to 8.5  $\mu\text{m}$ . For SHG measurements, the 1.06- $\mu\text{m}$  beam with 3 mJ/pulse was focused to a 1-mm spot on the sample and the reflected second-harmonic output was detected. To reduce fluctuations, the signal was normalized against a simultaneously measured SHG signal from a reference sample. For SFVS measurements, the 0.53- $\mu\text{m}$  beam and tunable IR beam with beam diameters of 1 and 0.5 mm and pulse energies of 1.5 mJ and 70  $\mu\text{J}$ , respectively, were overlapped on the sample and the reflected SF output was recorded. A SFVS vibrational spectrum would result when the IR input frequency scanned over the H-Si stretch mode. Our spectral resolution was limited by the input IR linewidth, which was  $\sim 6\text{ cm}^{-1}$ . All fields were *p*-polarized in the measurements.

The sum-frequency output is proportional to the absolute square of the surface nonlinear susceptibility  $\chi^{(2)}$ ,

$$S(\omega_{\text{IR}}) \propto |\chi^{(2)}(\omega_{\text{IR}})|^2 \quad (1)$$

with

$$\chi^{(2)} = \chi_{\text{NR}}^{(2)} + \chi_{\text{R}}^{(2)}, \quad (2)$$

$$\chi_{\text{R}}^{(2)} = \sum_q \frac{A_q}{(\omega_{\text{IR}} - \omega_q + i\Gamma_q)} \quad (3)$$

where  $\chi_{\text{R}}^{(2)}$  and  $\chi_{\text{NR}}^{(2)}$  are the resonant and nonresonant parts of the nonlinear susceptibility,  $\omega_{\text{IR}}$  is the input IR frequency, and  $\omega_q$ ,  $A_q$ , and  $\Gamma_q$  are the frequency, strength, and damping constant of the  $q$ th resonant mode, respectively. If  $\Gamma_q$  is much smaller than the input IR linewidth [as in the case of a well-ordered H termination of Si(111) surface], then it should be replaced by the latter in Eq. (3). More generally, a spectral convolution of  $\chi^{(2)}(\omega_{\text{IR}})$  with the input IR spectrum must be taken. For a given spectrum, fitting of the spectrum by Eqs. (1–3) allows a determination of the various parameters.

For a well-ordered H/Si(111),  $A_q$  is proportional to the H-surface coverage. In our measurements, we normalized the deduced  $A_q$  against that for a wet-chemically etched Si(111)-(1 $\times$ 1) sample, which has a full H coverage of  $8 \times 10^{14}/\text{cm}^2$ . At high temperatures, the H-Si vibrational resonance becomes very broad and weak because of the increased damping  $\Gamma_q$ . To avoid complication, all SFVS spectra in this work were taken at room temperature. On the other hand, the temperature dependence of SHG was not very strong and can be readily included in the analysis. Therefore, SHG was used in our experiment to follow the variation of H coverage even at high temperatures. However, SHG responds sensitively to the presence of dangling bonds, and decreases rapidly as H adsorbs on the surface to reduce the number of dangling bonds. Therefore, it is useful only for low-coverage measurements. At high coverage, surface-structural change further complicates the SHG result. In this work, we focus more on adsorption at low coverage.

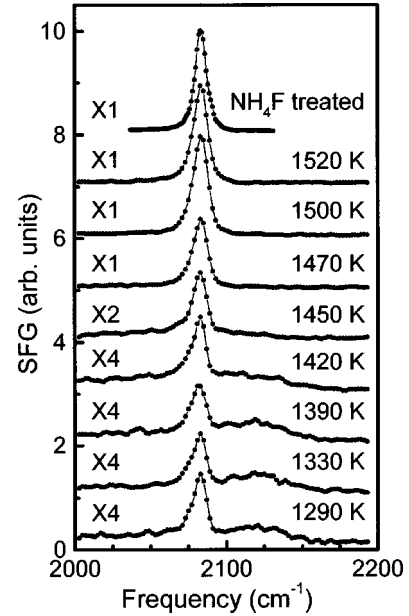


FIG. 1. SFVS vibrational spectra in the H-Si stretch region for H-terminated Si(111) surfaces prepared by flash heating to different temperatures. The spectrum from a wet-chemically etched Si(111) surface is also shown for comparison.

### III. RESULTS AND DISCUSSION

#### A. Dependence of SFVS spectrum on sample preparation

The SFVS surface vibrational spectrum of H/Si(111) appears to depend rather critically on sample preparation, namely, initial surface cleaning and hydrogen-dosing conditions. In an earlier publication,<sup>13</sup> we reported how the spectrum changed with the flash-heating temperature for surface cleaning of the bare Si surface. For convenience of discussion, we reproduce the results here in Fig. 1. The H<sub>2</sub> dosing condition ( $T=900\text{ K}$  and  $P=3.5\text{ Torr}$  for 5 min) was the same in all cases. If the flash-heating temperature of the sample was lower than 1420 K, the H-Si stretch peak at 2084  $\text{cm}^{-1}$  (associated with H at top sites) was relatively weak and a small dihydride peak appeared at 2130  $\text{cm}^{-1}$ , as seen in Fig. 1. Repeating the heating and H<sub>2</sub>-dosing procedure did not change or improve the spectrum. At higher flash-heating temperatures, the monohydride peak grew rapidly and the dihydride one dropped. Above 1500 K, the spectrum stabilized to a single sharp peak at 2084  $\text{cm}^{-1}$ , equal in quality to that of a H/Si(111)-(1 $\times$ 1) surface prepared by the wet-chemical-etching method (also shown in Fig. 1 for comparison).

The original purpose of flash heating to temperature above 1470 K was to remove carbon contamination on Si surfaces.<sup>28</sup> In our case, carbon contamination might be the reason for the deteriorated spectra obtained from flash heating at lower temperature, although it was found to be less than a few percent of a monolayer (ML). We also do not understand why it would be responsible for the appearance of the dihydride peak. In all cases, the (7 $\times$ 7) LEED patterns appeared identical. We believe that the Si surface flash

heated to above 1500 K was at least well ordered locally, although it might get macroscopically roughened by repeated flash heating.

In addition to the importance of temperature for flash cleaning, the H<sub>2</sub>-dosing temperature is also crucial. We found that to obtain a full monolayer of H on Si(111), the dosing temperature must be above 900 K. Sufficiently high H<sub>2</sub> pressure was also necessary in order to have adsorption overcome desorption at such high temperatures. The pressure was kept on to avoid H desorption when the sample was cooled. Below 900 K, a full-monolayer H coverage could not be reached even with dosing at 10 Torr for more than 1 h. We note that to our knowledge, realization of ideally hydrogen-terminated Si(111)-(1×1) surfaces by H<sub>2</sub> dosing has not been reported before.

### B. SHG for *in situ* measurements of H surface coverage

Although less specific than SFVS, surface SHG with the pump beam at 1.06 μm is particularly sensitive to suppression of Si dangling bonds, and is therefore more suitable for *in situ* probing of H adsorption on Si at low coverage. For an initially bare Si(111)-(7×7) surface, the maximum H coverage is ~0.4 ML (19 adsorption sites/49 surface Si atoms—this coverage is defined as 1 ML in Refs. 11 and 18) if the surface structure remains unchanged. With surface-structural change from (7×7) to (1×1),<sup>29</sup> the SHG response changes accordingly,<sup>30,31</sup> and becomes more complex as a probe for H-surface coverage. In our study of the early-stage adsorption kinetics of H on Si(111), to be discussed later, we only had to be concerned about the low-coverage regime.

We used the SFVS spectra to calibrate the SHG response to H coverage in our measurements. The former used the spectrum for a wet-chemically etched Si(111) surface as a reference of 1 ML of adsorbed H. Figure 2 shows the measured nonlinear susceptibility of SHG versus H coverage up to 0.35 ML, obtained by H<sub>2</sub> dosing at 640 K. The data are well described by an exponential function of the form

$$\chi^{(2)} = \chi_0 [1 - b + b \exp(-a\theta)] \quad (4)$$

where  $\chi_0$  is the nonlinear susceptibility of the bare Si surface and  $\theta$  is the H-surface coverage. In the low-coverage range, Eq. (4) becomes

$$\chi^{(2)} = \chi_0 (1 - \alpha\theta) \quad (5)$$

with  $\alpha = ab$ . This is the same expression used by Höfer and co-workers,<sup>11,12,18</sup> although our value of  $\alpha$  is about two times larger than theirs. The difference is likely due to the different input/output polarizations used (*p* in/*p* out in our case), but also could be due to different calibration procedures or sample preparations.

The parameters  $a$  and  $b$  generally depend on the sample temperature. Figures 2(b) and 2(c) depict the temperature dependence of  $a$  and  $b$ . They were obtained by measuring the SHG for a given H coverage as the sample cooled down. In agreement with Höfer and co-workers, the temperature dependence appeared to be rather weak in the limited temperature region. For temperatures above 640 K, we simply used extrapolation to find the temperature dependence of  $a$  and  $b$ .

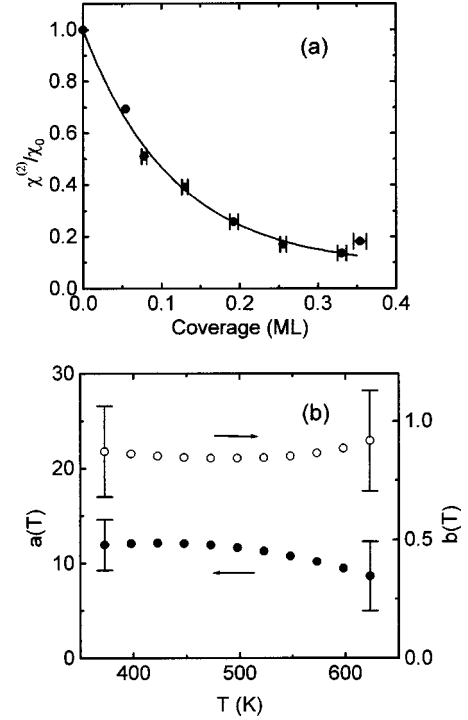


FIG. 2. (a) Normalized surface nonlinear susceptibility for SHG from H/Si(111) versus H surface coverage at  $T=640$  K. (b) Temperature dependence of  $a$  and  $b$  in Eq. (4).

### C. Adsorption at low temperatures

We used SHG to monitor *in situ* H<sub>2</sub> dissociative adsorption on Si(111) as a function of time. At sample temperatures significantly below the desorption temperature (~850 K), H desorption from Si is negligible, and hence the H coverage  $\theta(t)$  on Si simply results from the time-integrated H adsorption.

Figure 3(a) shows H coverage as a function of molecular-H<sub>2</sub> exposure dosed at 640 K sample temperature. The adsorption appeared to have two stages. During the first stage, H coverage increased rapidly from zero to 0.1 ML with molecular-hydrogen exposure. Then in the second stage, it increased much more slowly and eventually approached a saturation value. This seems to suggest the existence of two adsorption sites on the surface with significantly different kinetics, each obeying a Langmuir-type behavior.<sup>32</sup>

Figure 3(b) shows that the experimental results of adsorption at H coverage <0.1 ML fit very well with a simple second-order Langmuir adsorption model in which the H adsorption rate is given by<sup>33</sup>

$$K_{\text{ads}} = \frac{d\theta}{dt} = 2S_0(T)(1 - \theta/\theta_0)^2\Phi, \quad (6)$$

the integration of which yields

$$\theta(t) = \frac{2\theta_0 S_0(T)\Phi t}{\theta_0 + 2S_0(T)\Phi t} \quad (7)$$

where  $S_0(T)$  is the initial sticking coefficient that depends on temperature,  $\theta_0$  denotes an apparent saturation coverage, and

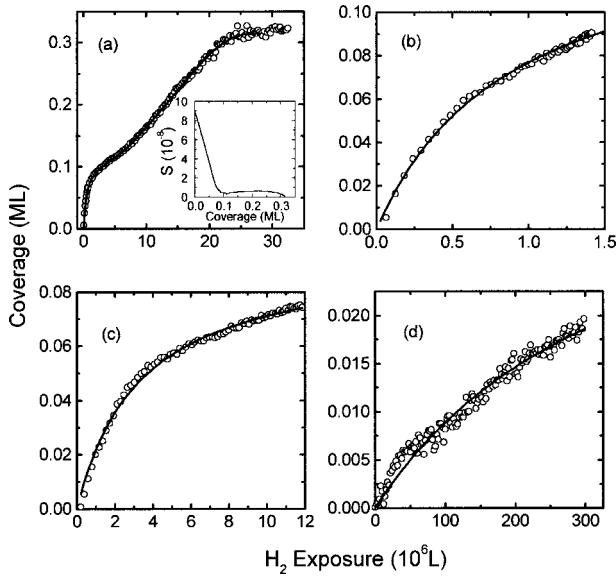


FIG. 3. H coverage on Si(111) versus exposure to H<sub>2</sub> at three different temperatures: (a) 640 K, (b) low-coverage range at 640, (c) 590, and (d) 480 K. The inset in (a) shows the sticking coefficient  $S$  versus H coverage.

$\Phi = p/[2\pi mk_B T_g]^{1/2}$  is the flux of the H<sub>2</sub> molecules of mass  $m$  with gas pressure  $p$  and gas temperature  $T_g$ . The factor 2 in Eq. (6) accounts for the fact that each H<sub>2</sub> molecule provides two H atoms when dissociated. The Langmuir behavior is also true for lower-dosing sample temperatures of 590 K and 480 K, shown in Fig. 3(c) and (d), respectively.

The sticking coefficient at finite coverage is defined by  $S(\theta) = K_{\text{ads}}/(2\Phi)$ . For the sample dosed at 640 K, the inset of Fig. 3(a) shows that  $S$  exhibits a complex behavior in its dependence on H coverage. It decreases with increasing H coverage up to 0.1 ML and then increases slightly until 0.25 ML, after which it decays to zero. For  $\theta < 0.1$  ML, we have  $S(\theta) = S_0(1 - \theta/\theta_0)^2$ . This is different from what Bratu *et al.* observed.<sup>18</sup> They found that at  $\sim 640$  K,  $S(\theta)$  initially increased with  $\theta$  near  $\theta = 0$  and suggested a cooperative adsorption mechanism to explain the result.

The fit of the data in Fig. 3 by Eq. (7) yielded values of  $\theta_0$  smaller than 1. The lower the dosing temperature, the smaller is the value of  $\theta_0$ . For  $T = 480, 530, 590,$  and  $640$  K, we found  $\theta_0 = 0.042, 0.049, 0.095,$  and  $0.146$ , respectively. This suggests that H<sub>2</sub> dissociative adsorption is not a simple Langmuir-adsorption process governed by site blocking. The requirement of simultaneous adsorption of H pairs at two neighboring sites and slower diffusion of adsorbates at lower temperature must have an effect on the adsorption kinetics, as we shall discuss later.

#### D. Adsorption at high temperatures

At sample temperatures close to or higher than the desorption temperature, H desorption from the sample surface cannot be neglected during adsorption. As a function of time, the H-surface coverage is given by

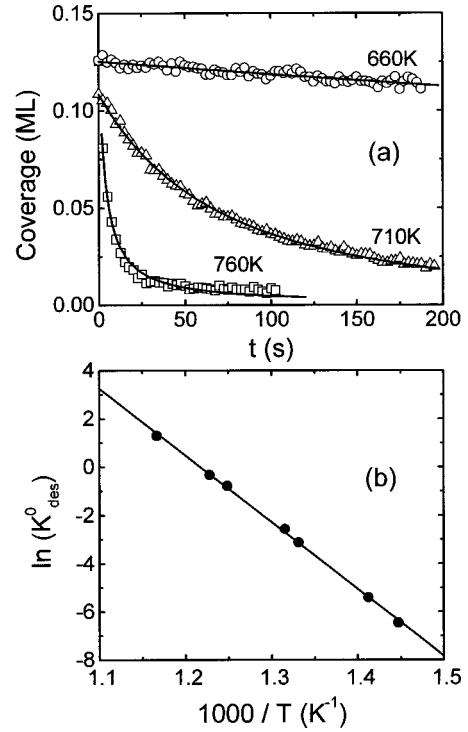


FIG. 4. (a) Typical data showing reduction of H coverage on Si(111) by thermal desorption at three different temperatures: 660 (circles), 710 (triangles), and 760 K (squares). The solid curves are fits to Eq. (9) (with  $m = 1.5$ ) from which the values of the decay coefficient  $K_{\text{des}}^0$  are deduced. (b) Plot of  $(\ln K_{\text{des}}^0)$  versus the inverse temperature. The slope of the straight line yields the value of the desorption energy barrier,  $E_d = 2.38$  eV.

$$\theta(t) = \int_0^t (K_{\text{ads}} - K_{\text{des}}) dt \quad (8)$$

with

$$K_{\text{des}} = \theta(t)^m K_{\text{des}}^0(T) = \theta(t)^m \nu \exp(-E_d/k_B T) \quad (9)$$

where  $K_{\text{ads}}$  is given in Eq. (6),  $K_{\text{des}}$  is the desorption rate with  $\nu$  and  $E_d$  being the preexponential and desorption energy, respectively, and  $m$  denotes the desorption order. At equilibrium,  $K_{\text{ads}} = K_{\text{des}}$  and hence

$$2\Phi S(\theta, T) = \theta^m \nu \exp(-E_d/k_B T) \quad (10)$$

from which  $S(\theta, T)$  can be deduced if  $m$ ,  $\nu$ , and  $E_d$  for desorption are known.

Hydrogen desorption from Si(111) has been carefully studied by Reider, Höfer, and Heinz using SHG.<sup>34</sup> They found  $m = 1.5$  and  $E_d = 2.4$  eV. We repeated the measurements on our sample. Figure 4 shows the data of isothermal desorption at temperatures of (a) 660, (b) 710, and (c) 760 K. They can all be well described by Eq. (10) with  $m = 1.5$ . A plot of  $\ln(K_{\text{des}}^0)$  versus  $1/T$  in Fig. 4(b) yields a value of  $2.38 \pm 0.13$  eV for  $E_d$ , in agreement with the value obtained by Reider, Höfer, and Heinz. As suggested by Reider, Höfer, and Heinz, the result of  $m = 1.5$  can be explained by the presence of two adsorption sites for H on Si with different diffusion and recombination properties. At higher sample

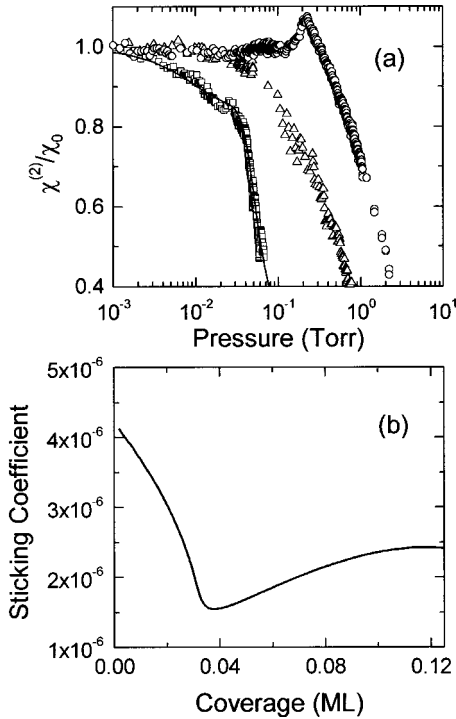


FIG. 5. (a) Measured surface nonlinear susceptibility as a function of  $\text{H}_2$  gas pressure at three different temperatures: 860 (squares), 930 (triangles), and 980 K (circles). (b) Conversion of data at 860 K in (a) to the sticking coefficient versus coverage.

temperatures, desorption is faster and diffusion less important; accordingly, Eq. (10) with  $m=1$  becomes a reasonable approximation to describe the major portion of the desorption process. At temperatures higher than the desorption temperature, desorption of H from Si is too fast for us to carry out an isothermal desorption measurement. We then simply assume that Eq. (10) is still valid with  $m=1$ .

Figure 5(a) displays the measured nonlinear susceptibility of SHG as a function of  $\text{H}_2$  gas pressure for H/Si(111) dosed at 860, 930, and 980 K. The data for H/Si(111) dosed at 860 K is converted to  $\theta$  versus  $p$  using Eq. (4), and then  $S(\theta)$  versus  $\theta$  using Eq. (10) with  $m=1$ , and is presented in Fig. 5(b). It is seen that the sticking coefficient  $S(\theta)$  first decreases with  $\theta$  up to 0.04 ML, and then increases with  $\theta$ . This is similar to the behavior at low temperatures [see Fig. 3(a), inset] except that the turnaround coverage is smaller and the coverage increase is faster in the subsequent stage. It seems that the cooperative adsorption mechanism suggested by Bratu *et al.*<sup>18</sup> becomes more effective at higher temperatures. However, we believe that this is probably because of the surface-structural change, which is more readily induced by H adsorbates at higher temperature, as we shall discuss later.

### E. Initial sticking coefficient versus temperature

The initial sticking coefficient  $S_0$  is defined as the sticking probability on a bare surface ( $\theta=0$ ). At low temperatures, it can be deduced directly from the initial slope of the adsorption curve,  $\theta(t)$ . At high temperatures, it can be obtained from extrapolation of  $S(\theta)$  to  $\theta=0$ . Figure 6 shows the plot

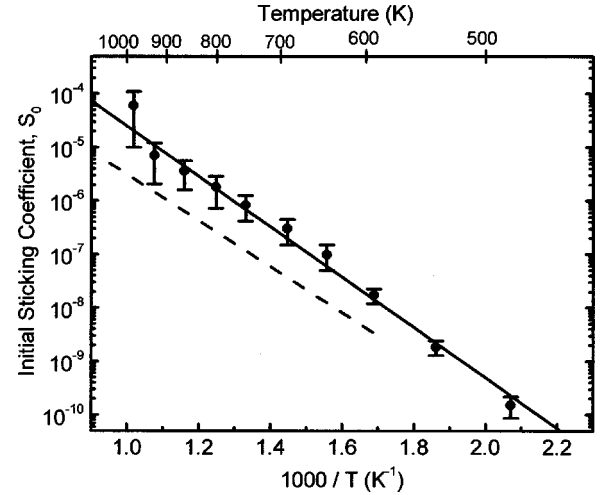


FIG. 6. Deduced initial sticking coefficient as a function of inverse temperature in a semilog plot. The slope of the solid line that fits the data yields the value of the adsorption-energy barrier,  $E_{\text{ad}}=0.94$  eV. The dashed line is the result obtained by Bratu and Höfer in Ref. 11.

of  $\log(S_0)$  versus  $1/T$  deduced from our measurements. The data can be described by a straight line that takes the form  $S_0 \propto \exp(-E_{\text{ad}}/k_B T)$ . The slope of the line then yields an activation-energy barrier  $E_{\text{ad}}=0.94 \pm 0.1$  eV. It agrees well with the value of  $0.9 \pm 0.1$  eV obtained by Bratu and co-workers,<sup>11,12,18</sup> but our value of  $S_0$  is several times larger.

We note here that because the sticking coefficients of  $\text{H}_2$  on Si are small, they are difficult to measure accurately. For example, the sticking coefficients for  $\text{H}_2$  on Si(100) obtained by Kolasinski *et al.*<sup>17</sup> and Bratu and co-workers<sup>12,18</sup> differ by up to four orders of magnitude. The controversy was only recently resolved by Durr, Raschke, and Höfer<sup>35</sup> and the smaller values of Bratu *et al.* were recently confirmed by Zimmermann and Pan.<sup>36</sup> For  $\text{H}_2$  on Si(111), the results of Hansen, Halbach, and Seebauer<sup>37</sup> on slightly misoriented surfaces differ from those of Raschke and Höfer<sup>38</sup> and Bratu *et al.* (on flat surface) by more than five orders of magnitude. Therefore, we consider it most remarkable that our initial sticking coefficients disagree with those of Bratu and Höfer<sup>11</sup> by only a few times in the preexponential factor, despite the difference in coverage dependence.

### F. Surface-structural change during hydrogen adsorption

The bare Si(111) surface below 1130 K has a  $(7 \times 7)$  structure, but the H-terminated surface has a  $(1 \times 1)$  structure. Therefore, a surface-structural transition from  $(7 \times 7)$  to  $(1 \times 1)$  should take place during adsorption as the H coverage increases. For a bare Si(111) surface, the surface reconstructs at 1130 K in ultrahigh vacuum.<sup>29-31</sup> With adsorption of H, it must occur at lower temperatures. The evidence of a surface structural change is actually visible in Fig. 5(a) (open circle) describing SHG versus  $\text{H}_2$  gas pressure at the sample temperature of 980 K. Without surface-structural change, SHG should decrease monotonically with increase of H coverage (or pressure). The data in Fig. 5(a) for hydrogen dosed at 980 K shows a sudden increase at  $P \sim 0.2$  Torr instead.

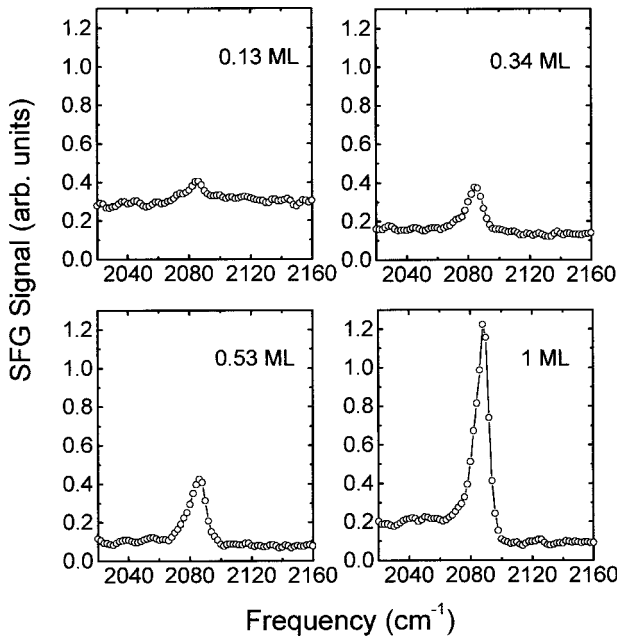


FIG. 7. SFVS spectra of the H-Si stretch mode of H/Si(111) at four different H coverages, obtained by H<sub>2</sub> dosing at 900 K.

The result in Fig. 5(a) shows that at 980 K, surface-structural transition occurs with a H coverage barely detectable. At lower temperatures, it would take place at higher H coverage, but we could not detect any evidence in our SHG data in Figs. 3 and 5. We believe that this is because H coverage on the surface is not necessarily uniform so that the surface-structural transition would first nucleate and form microdomains, and then spread over the entire surface. Hence, the corresponding change of SHG would be gradual rather than sudden. It is also partly because at higher H coverage, SHG is weaker and less sensitive to detect changes.

Contrary to SHG, the SFVS spectral peak is more sensitive to higher H coverage, and more suitable to monitor surface-structural changes at higher H coverage. Figures 7 and 8 present the spectra for different H coverage obtained by dosing at two different sample temperatures. At 900 K (Fig. 7), the spectral peak intensity varies with coverage but the spectral shape remains unchanged. This indicates the absence of surface-structural transition in the coverage range studied. The Si(111) surface must have transformed from (7×7) to (1×1) before the H coverage reached 0.13 ML. At 640 K, both the peak strength and the spectral shape change significantly with coverage. The spectral shape changes from an absorptionlike peak to a dispersionlike peak. This is due to change in the phase of the nonresonant background [ $\chi_{\text{NR}}^{(2)}$  in Eq. (2)], which comes mainly from the dangling bonds at the surface. While the magnitude of  $\chi_{\text{NR}}^{(2)}$  can be affected by H coverage, the phase of  $\chi_{\text{NR}}^{(2)}$  can only be affected by change of surface structure. Thus we believe that the continuous change of the spectral shape with H coverage on Si(111) at 640 K, displayed in Fig. 8, is an indication of a continuous surface-structural change induced by H adsorption [i.e., continuous increase of surface fraction

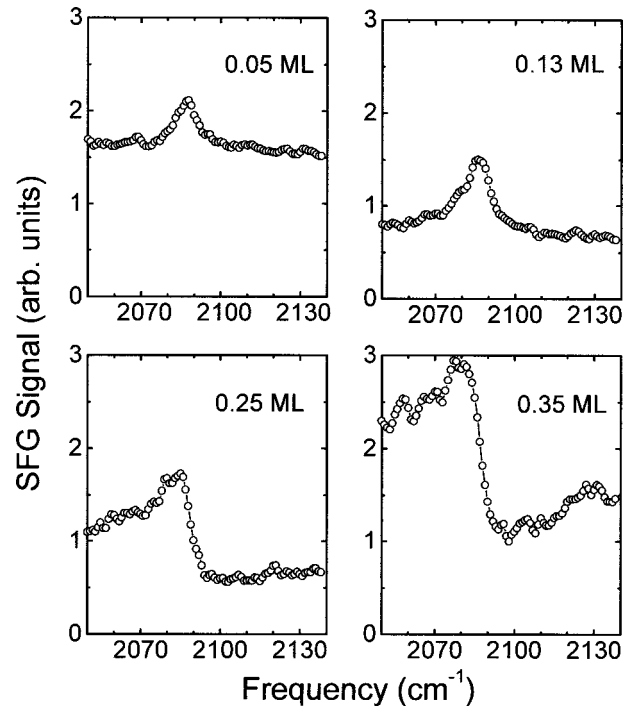


FIG. 8. SFVS spectra of the H-Si stretch mode of H/Si(111) at four different H coverages, obtained by H<sub>2</sub> dosing at 640 K.

changed from (7×7) to (1×1)]. At even lower temperatures with H coverage limited to 0.1 ML, the spectra shape again did not change with coverage presumably because surface transition from (7×7) to (1×1) had never occurred.

The results in Fig. 8 from H/Si(111) at 640 K show that the spectral shape started to change at coverage of about 0.1 ML. It agrees with the coverage at which  $S(\theta)$  begins to increase, as shown in Fig. 3(a). This suggests that the observed complex-adsorption behavior is likely due to surface-structural change during hydrogen adsorption.

### G. Adsorption model

Dissociative adsorption of H<sub>2</sub> on Si(111) has been studied theoretically by a number of authors.<sup>18,20,39</sup> On the Si(111)-(7×7) surface, the process is well explained by the ‘‘phonon-assisted’’ pair-adsorption model.<sup>18</sup> Vittadini and Selloni<sup>19</sup> and Cho, Kaxiras, and Joannopoulos<sup>20</sup> have identified the process of lattice distortion and adatom-backbond breaking as the mechanism that determines the adsorption-energy barrier. Regarding the coverage dependence, we have found that at low coverage, the adsorption behavior is of the Langmuir type, but at high coverage, it is of the cooperative type. Explanation of the results apparently requires an extension of the above-mentioned model and surface-structural change should play a role.

The observed coverage dependence of the sticking coefficient suggests that there exist two types of adsorption sites. At low temperatures or/and coverages, one would be predominantly occupied, but at high temperature or/and coverages, the other would become accessible. One possible sce-

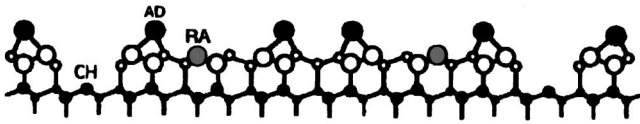


FIG. 9. A side view of the Si(111)-(7 $\times$ 7) dimer-adatom-stacking fault model surface. AD, RA, and CH denote the adatom (large black dots), rest atom (large gray dots), and the corner-hole dangling bond sites (adapted from Ref. 25).

nario is that our 1500-K flash heating had created a surface with many steps and other defect sites. As reported by Raschke and Höfer,<sup>38</sup> dissociative H<sub>2</sub> adsorption more readily occurs at defect sites than at terrace sites. At low temperatures, adsorption at defect sites would dominate and show Langmuir-type behavior with a low saturation coverage. At sufficiently higher temperatures, diffusion of H from defect sites to terrace sites would become significant and the apparent saturation coverage would become higher accordingly. However, diffusion of H from defect sites to terrace sites is presumably slower than that on terrace sites, which was measured by Reider, Höfer, and Heinz.<sup>40</sup> We would expect it to be not appreciable in the temperature range where data of Fig. 3 were taken. The Langmuir-type saturation coverage would then be independent of temperature, but this is not what we observed. Another fact is that in this temperature range, our measured initial sticking coefficients fall together with the high-temperature data points nicely on the Arrhenius plot in Fig. 6 that determines the adsorption-energy barrier, suggesting that the responsible adsorption sites are characteristically not very different from the terrace sites. Therefore, it is difficult to conceive that they are the defect sites.

We offer here another plausible model. As shown in Fig. 9, the Si(111)-(7 $\times$ 7) surface structure has a dimer-adatom-stacking fault pattern.<sup>25,41</sup> The dangling bonds at the surface are associated with three different kinds of surface Si atoms, namely, adatoms (AD), rest atoms (RA), and corner-hole (CH) atoms. In each 7 $\times$ 7 unit, there are 6 dangling bonds at RA sites, 12 at AD sites, and 1 at the CH site. We shall neglect CH in our discussion because its involvement in the dissociative adsorption would increase the adsorption-energy barrier significantly. At low temperatures and low coverage, the Si(111)-(7 $\times$ 7) surface structure remains unchanged.<sup>42</sup> Hydrogen adsorption is dominated by dissociative adsorption at neighboring AD-RA empty sites since they have the shortest distance between them and hence the lowest adsorption-energy barrier.<sup>20</sup> Adsorption will be greatly hindered if all the six RA sites are occupied, although there still exist six empty AD sites. Further adsorption can occur if H atoms at the RA sites diffuse away, leaving AD-RA pair sites open again. In this case, the adsorption is limited by the H diffusion rate, which increases with increase of temperature.<sup>42</sup> This explains qualitatively the Langmuir-type adsorption behavior with a saturation coverage depending on temperature.

As the H coverage increases, it tends to promote the surface-structural change from (7 $\times$ 7) to (1 $\times$ 1) and thus create more dangling-bond pair sites for adsorption. In a recent transmission-electron diffraction experiment,<sup>43</sup> it was

found that after a (7 $\times$ 7) surface had been exposed to hydrogen, some of the adatoms disappeared. Presumably H<sub>2</sub> adsorption had significantly weakened the backbonds of the AD and allowed it to diffuse away or desorb. Removal of one AD would create three dangling bonds in the RA layer and therefore additional pair sites for adsorption. The distance between the newly created neighboring sites is shorter than that of the AD-RA pair. This would lead to a lower adsorption-energy barrier because a smaller lattice distortion is needed to assist the H<sub>2</sub> adsorption. The increasing number of adsorption sites and the lower energy barrier from AD removal, enhance the adsorption and cause the adsorption kinetics to deviate from the simple Langmuir type to the cooperative type. Since removal of adatoms is a temperature-dependent process, this type of transition occurs at lower coverage if the temperature is higher, and it allows the saturation coverage to reach a full monolayer if the surface is dosed at sufficiently high temperature. Removal of AD may also be the step that initiates the adsorption-induced surface-structural change from (7 $\times$ 7) to (1 $\times$ 1).

#### IV. CONCLUSION

We have used SFVS to probe the H-Si stretch mode and characterize the H/Si(111) surface. We found that it was possible to obtain a fully covered H/Si(111)-(1 $\times$ 1) surface by molecular-hydrogen dosing if the dosing temperature was above 900 K. The H-terminated surface had a quality as good as that of a wet-chemically etched surface if, before dosing, the bare surface had been cleaned by flash heating to above 1500 K. We used optical SHG to probe H<sub>2</sub> dissociative adsorption on such a surface. The observed adsorption kinetics was qualitatively the same as that observed by Höfer and co-workers. The adsorption-energy barrier was nearly the same although our values of the sticking coefficients were a few times higher. In the low-coverage range, the adsorption kinetics obeyed a simple Langmuir model with the sticking coefficient decreasing with coverage, but if the temperature was sufficiently high, the sticking coefficient appeared to increase in a certain high-coverage range, suggesting the occurrence of a thermally induced cooperative adsorption process. Both SHG and SFVS results showed evidence of surface-structural transition from (7 $\times$ 7) to (1 $\times$ 1) at sufficiently high temperature and coverage. We incurred the possibility of adsorption-induced removal of adatoms in a simple physical model to explain our observation qualitatively.

#### ACKNOWLEDGMENTS

We would like to acknowledge many helpful discussions with Markus Raschke. This work was supported by the Director, Office of Energy Research, Office of Basic Energy Sciences, Materials Science Division, of the U.S. Department of Energy under Contract No. DE-AO03-76SF00098.



- \*Present address: Polymer Institute, University of California, Santa Barbara, CA 93106.
- †Present address: Department of Physics, Sogang University, Seoul 100-611, Korea.
- ‡Corresponding author. Email address: shenyr@socrates.berkeley.edu
- <sup>1</sup>H. Ibach and J. E. Rowe, *Surf. Sci.* **43**, 481 (1974).
- <sup>2</sup>T. Sakurai and H. D. Hagstrum, *Phys. Rev. B* **12**, 5349 (1975).
- <sup>3</sup>E. G. McRae and C. W. Caldwell, *Phys. Rev. Lett.* **46**, 1632 (1981).
- <sup>4</sup>G. Schulze and M. Henzler, *Surf. Sci.* **124**, 336 (1983).
- <sup>5</sup>Y. J. Chabal, G. S. Higashi, and S. B. Christman, *Phys. Rev. B* **28**, 4472 (1983).
- <sup>6</sup>B. G. Koehler, C. H. Mak, D. A. Arthur, P. A. Coon, and S. M. George, *J. Chem. Phys.* **89**, 1709 (1988).
- <sup>7</sup>C. J. Karlsson, E. Landemark, L. S. O. Johansson, U. O. Karlsson, and R. I. G. Uhrberg, *Phys. Rev. B* **41**, 1521 (1990).
- <sup>8</sup>K. Mortensen, D. M. Chen, P. J. Bedrossian, J. A. Golovchenko, and F. Besenbacher, *Phys. Rev. B* **43**, 1816 (1991).
- <sup>9</sup>K. W. Kolasinski, W. Nessler, A. de Meijere, and E. Hasselbrink, *Phys. Rev. Lett.* **72**, 1356 (1994).
- <sup>10</sup>F. Owman and P. Martensson, *Surf. Sci.* **324**, 211 (1995).
- <sup>11</sup>P. Bratu and U. Höfer, *Phys. Rev. Lett.* **74**, 1625 (1995).
- <sup>12</sup>P. Bratu, K. L. Kompa, and U. Höfer, *Chem. Phys. Lett.* **251**, 1 (1996).
- <sup>13</sup>M. Y. Mao, P. B. Miranda, D. S. Kim, and Y. R. Shen, *Appl. Phys. Lett.* **75**, 3357 (1999).
- <sup>14</sup>G. S. Higashi, Y. J. Chabal, G. W. Trucks, and K. Raghavachari, *Appl. Phys. Lett.* **56**, 656 (1990).
- <sup>15</sup>P. Dumas, Y. J. Chabal, and G. S. Higashi, *Phys. Rev. Lett.* **65**, 1124 (1990).
- <sup>16</sup>P. Avouris, F. Bozso, and R. J. Hamers, *J. Vac. Sci. Technol. B* **5**, 1387 (1987).
- <sup>17</sup>K. W. Kolasinski, W. Nessler, K.-H. Bornscheuer, and E. Hasselbrink, *J. Chem. Phys.* **101**, 7082 (1994).
- <sup>18</sup>P. Bratu, W. Brenig, A. Gross, M. Hartmann, U. Höfer, P. Kratzer, and R. Russ, *Phys. Rev. B* **54**, 5978 (1996).
- <sup>19</sup>A. Vittadini and A. Selloni, *Surf. Sci. Lett.* **383**, L779 (1997).
- <sup>20</sup>K. Cho, E. Kaxiras, and J. D. Joannopoulos, *Phys. Rev. Lett.* **79**, 5078 (1997).
- <sup>21</sup>L. T. Vinh, M. Eddrief, C. A. Sébenne, P. Dumas, A. Tableb-Ibrahimi, R. Gunther, Y. J. Chabal, and J. Derrien, *Appl. Phys. Lett.* **64**, 3308 (1994).
- <sup>22</sup>M. C. Flowers, N. B. H. Jonathan, A. Morris, and S. Wright, *J. Chem. Phys.* **108**, 3342 (1998).
- <sup>23</sup>M. Naitoh, H. Shimaya, A. Watanabe, and S. Nishigaki, *Jpn. J. Appl. Phys., Part 1* **37**, 2033 (1998).
- <sup>24</sup>Y. Tanaka, K. Ishiyama, and A. Ichimiya, *Surf. Sci.* **357/358**, 840 (1996).
- <sup>25</sup>I-S. Hwang, R.-L. Lo, and T. T. Tsong, *Phys. Rev. Lett.* **78**, 4797 (1997).
- <sup>26</sup>J. H. Hunt, P. Guyot-Sionnest, and Y. R. Shen, *Chem. Phys. Lett.* **133**, 189 (1987).
- <sup>27</sup>Y. R. Shen, *Surf. Sci.* **299/300**, 551 (1994).
- <sup>28</sup>R. C. Henderson, W. J. Polito, and J. Simpson, *Appl. Phys. Lett.* **16**, 15 (1970).
- <sup>29</sup>P. A. Bennett and M. W. Webb, *Surf. Sci.* **104**, 74 (1981).
- <sup>30</sup>U. Höfer, L. Li, R. A. Ratzlaff, and T. F. Heinz, *Phys. Rev. B* **52**, 5264 (1995).
- <sup>31</sup>T. Suzuki, A. Mikami, Y. Kimura, K. Uehara, and M. Aono, *Surf. Sci.* **357/358**, 107 (1996).
- <sup>32</sup>M. Raschke, Ph.D. thesis, Technical University of Munich, 1999.
- <sup>33</sup>A. Zangwill, *Physics at Surfaces* (Cambridge University Press, New York, 1988).
- <sup>34</sup>G. A. Reider, U. Höfer, and T. F. Heinz, *J. Chem. Phys.* **94**, 4080 (1991).
- <sup>35</sup>M. Durr, M. B. Raschke, and U. Höfer, *J. Chem. Phys.* **111**, 10 411 (1999).
- <sup>36</sup>F. M. Zimmermann and X. Pan, *Phys. Rev. Lett.* **85**, 618 (2000).
- <sup>37</sup>D. A. Hansen, M. R. Halbach, and E. G. Seebauer, *J. Chem. Phys.* **104**, 7338 (1996).
- <sup>38</sup>M. Raschke and U. Höfer, *Appl. Phys. B: Lasers Opt.* **B68**, 649 (1999).
- <sup>39</sup>B. R. Wu, C. Chang, and S. L. Lee, *J. Phys. Chem. A* **101**, 6545 (1997).
- <sup>40</sup>G. A. Reider, U. Höfer, and T. F. Heinz, *Phys. Rev. Lett.* **66**, 1994 (1991).
- <sup>41</sup>K. Takayanagi, Y. Tanishiro, M. Takahashi, and S. Takahashi, *J. Vac. Sci. Technol. A* **3**, 1502 (1985).
- <sup>42</sup>R.-L. Lo, I-S. Hwang, M-S. Ho, and T. T. Tsong, *Phys. Rev. Lett.* **80**, 5584 (1998).
- <sup>43</sup>S. H. Wolff, S. Wagner, J. M. Gibson, D. Loretto, I. K. Robinson, and J. C. Bean, *Surf. Sci. Lett.* **239**, L537 (1990).